Braiding of Atomic Majorana Fermions in Wire Networks and Implementation of the Deutsch-Jozsa Algorithm

Christina V. Kraus,[1,2] P. Zoller,[1,2] and Mikhail A. Baranov[1,2,3]

[1]*Institute for Quantum Optics and Quantum Information of the Austrian Academy of Sciences, A-6020 Innsbruck, Austria*
[2]*Institute for Theoretical Physics, Innsbruck University, A-6020 Innsbruck, Austria*
[3]*RRC "Kurchatov Institute," Kurchatov Square 1, 123182 Moscow, Russia*

(Received 20 February 2013; published 11 November 2013)

We propose an efficient protocol for braiding Majorana fermions realized as edge states in atomic wire networks, and demonstrate its robustness against experimentally relevant errors. The braiding of two Majorana fermions located on one side of two adjacent wires requires only a few local operations on this side which can be implemented using local site addressing available in current experiments with cold atoms and molecules. Based on this protocol we provide an experimentally feasible implementation of the Deutsch-Jozsa algorithm for two qubits in a topologically protected way.

DOI: 10.1103/PhysRevLett.111.203001 PACS numbers: 37.10.Jk, 03.67.Lx, 03.67.Ac

The prediction of particles with anyonic statistics in topological phases of matter has resulted in the proposal of decoherence-free topological quantum computation (TQC) [1–3]. TQC requires the creation of anyonic particles as well as their controlled interchange, known as braiding, which is the fundamental building block of topological quantum gates [4,5]. While the implementation of these tasks in real physical systems is an outstanding challenge, the reported observation of anyonic Majorana fermions (MFs) in hybrid superconductor-semiconductor nanowire devices [6–8] and the proposals for the manipulation [9–11] of anyonic Majorana fermions in solid state systems are promising first steps in this direction [11–16]. A complementary and promising approach towards realizing and coherently controlling MFs are ultracold atoms confined to one-dimensional (1D) optical lattices coupled to BCS or molecular atomic reservoirs. The recent realization of a quantum gas microscope [17,18] for optical lattices adds single-site addressing and measurement to the toolbox of possible atomic operations to create and detect MFs [19–21].

Building on these experimental advances, we describe in this Letter an efficient braiding protocol for atomic MFs in a network of one-dimensional quantum wires (see Fig. 1), in which MFs appear as edge states (yellow and black spheres in Fig. 2). The protocol for braiding two MFs on one side of two adjacent wires requires only local operations on this side of the wires and can be completed in four time steps, during which adiabatic changes on the two edge sites and the nearby links are performed by local addressing (see Fig. 2). We demonstrate that our braiding protocol tolerates relevant experimental imperfections and, therefore, provides a realistic and practical way to probe the non-Abelian anyonic statistics of MFs. The braiding protocol can also be used as an elementary building block for TQC, which does not require the usage of a universal set of gates [22,23]. We show this by implementing the Deutsch-Jozsa algorithm [24] on two qubits via braiding only, demonstrating that the realization of simple topologically protected quantum algorithms in atomic setups is within experimental reach.

Braiding of atomic Majorana fermions.—We consider a system of single component fermions that are confined to an array of 1D wires of L sites (see Fig. 1) and that are governed by a Hamiltonian $H = \sum_n H^{(n)}$. The Hamiltonian $H^{(n)} = \sum_{j=1}^{L-1}(-J a^\dagger_{n,j} a_{n,j+1} + \Delta a_{n,j} a_{n,j+1} + \text{H.c.}) - \mu \sum_n a^\dagger_n a_n$ realizes a Kitaev chain [25] in the nth wire. The operators $a^\dagger_{n,j}$ and $a_{n,j}$ are fermionic creation and annihilation operators, $J > 0$ and $\Delta \in \mathbb{R}$ are nearest-neighbor hopping and pairing amplitudes, and μ is a chemical potential. As demonstrated in Ref. [19], a Hamiltonian of the form $H^{(n)}$ allows for a cold atom implementation: while the hopping term arises naturally in an optical lattice setup, the pairing term can be realized by a Raman induced dissociation of Cooper pairs (or Feshbach molecules) forming an atomic BCS (or BEC) reservoir. For an alternative experimental proposal see also

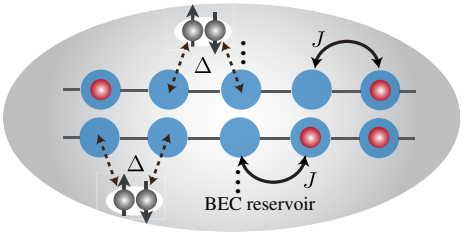

FIG. 1 (color online). Realization of an array of one-dimensional Kitaev wires in an optical lattice setup: atoms (red circles) can hop between neighboring sites (blue circles) with strength J along the individual wires. The pairing term of strength Δ can be realized by a Raman induced dissociation of Cooper pairs (or Feshbach molecules) forming an atomic BCS reservoir.

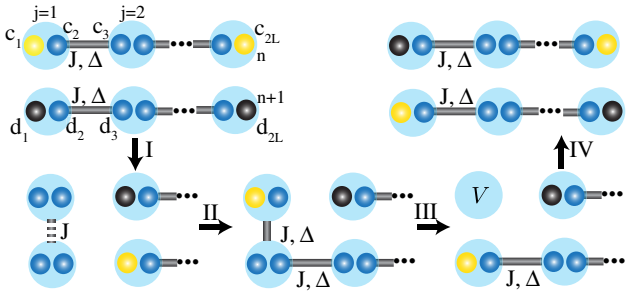

FIG. 2 (color online). Braiding protocol for two perfect quantum wires. The zero-energy Majorana modes that are initially on the upper (lower) wire are shown as yellow (black) spheres, while the blue ones correspond to the Majorana operators, which are coupled into finite-energy fermionic modes. Coupling of Majorana operators via hopping and pairing (Kitaev coupling) is indicated by gray solid links, while the coupling via hopping only is shown as a dashed link.

Ref. [20]. Estimates give tens of nanokelvins for the energy gap separating the Majorana states from the rest of the spectrum.

The Hamiltonian $H^{(n)}$ supports zero energy Majorana fermions of the form $\gamma^{(n)}_{L(R)} = \sum_j \upsilon^{L(R)}_{n,j} c_{n,j}$ with (real) coefficients $\upsilon^{L(R)}_{n,j}$, which are localized at the left (right) end of the nth wire (see Ref. [25]). Here, $c_{n,2j-1} = a^\dagger_{n,j} + a_{n,j}$ and $c_{n,2j} = (-i)(a^\dagger_{n,j} - a_{n,j})$ are Majorana operators fulfilling $\{c_{n,k}, c_{m,l}\} = 2\delta_{kl}\delta_{mn}$. For the "ideal" quantum wire ($J = |\Delta|$, $\mu = 0$), one has $\upsilon^{L}_{n,1} = 1$, $\upsilon^{R}_{n,2L} = 1$ and else $\upsilon^{L(R)}_{n,j} = 0$. Otherwise, the modes $\gamma^{(n)}_{L(R)}$ decay exponentially inside the bulk. Each wire has two degenerate ground states $|0_n\rangle$ and $|1_n\rangle$ with even and odd parity, respectively, corresponding to the presence or absence of the Majorana fermion $f_n = \gamma^{(n)}_L - i\gamma^{(n)}_R$, i.e., $f_n|0_n\rangle = 0$, $f^\dagger_n|0_n\rangle = |1_n\rangle$. For the preparation of MFs in the desired parity subspace see Ref. [21].

Due to the non-Abelian nature of MFs, the interchange of two Majorana modes γ_1 and γ_2 (braiding) gives rise to the transformation $\gamma_1 \mapsto -\gamma_2$, $\gamma_2 \mapsto \gamma_1$. This is equivalent to applying the unitary $U_b = e^{\pi\gamma_1\gamma_2/4}$, which is the key step for realizing a TQC. In the following we present a braiding protocol for a cold atom implementation of MFs. To this end, we consider two neighboring wires n and $n+1$ governed by two ideal Kitaev Hamiltonians $H^{(n)}$ and $H^{(n+1)}$. Although the protocol works equally well for general Kitaev Hamiltonians (see below), the use of ideal wires allows for a simple analytical treatment because only six Majorana operators on four sites are involved. If we label the sites by (w, j), where $w = u, l$ denotes the upper (n) and lower ($n+1$) wire, respectively, and $j = 1, \ldots, L$, then the sites involved are $\vec{s}_1 = (u, 1)$, $\vec{s}_2 = (u, 2)$, $\vec{s}_3 = (l, 1)$, and $\vec{s}_4 = (l, 2)$ (see Fig. 2). With the notation $c_{u,j} \equiv c_j$ and $c_{l,j} \equiv d_j$, the Majorana zero modes are $\gamma^{(u)}_L = c_1$, $\gamma^{(u)}_R = c_{2L}$, $\gamma^{(l)}_L = d_1$, and $\gamma^{(l)}_R = d_{2L}$.

Let us now show how to braid the left Majorana modes $\gamma^{(u)}_L$ and $\gamma^{(l)}_L$ with only local (adiabatic) changes in the Hamiltonian on the left edge of the system: switching on or off (i) the hopping $H^{(h)}_{\vec{s}_i,\vec{s}_j} = -Ja^\dagger_{\vec{s}_i} a_{\vec{s}_j}$ + H.c. and (ii) the pairing $H^{(p)}_{\vec{s}_i,\vec{s}_j} = Ja_{\vec{s}_i} a_{\vec{s}_j}$ + H.c. between the neighboring sites $\vec{s}_i$ and $\vec{s}_j$, and (iii) the local potential $H^{(lp)}_{\vec{s}_i} = 2Va^\dagger_{\vec{s}_i} a_{\vec{s}_i}$ on the site $\vec{s}_i$. Note that a combination of (i) and (ii) allows us to switch on or off the Kitaev coupling $H^{(K)}_{\vec{s}_i,\vec{s}_j} = H^{(h)}_{\vec{s}_i,\vec{s}_j} + H^{(p)}_{\vec{s}_i,\vec{s}_j}$. Experimentally, these operations can be achieved by changing the intensity of the laser field(s) on the corresponding site or link in a controllable way by using a combination of a high-resolution imaging system [17,26] and a spatial light modulator (see, e.g., Ref. [27]).

Braiding protocol.—The physical process behind the braiding is the transfer of one fermion from the system (either from the upper or from the lower wire) into, say, the lower wire. We characterize the required adiabatic changes via a time-dependent parameter ϕ_t that varies from 0 to $\pi/2$, and perform them in four steps. In describing these steps, we write down only the Hamiltonian for the four involved sites (the Hamiltonian for the rest of the wires remains unchanged) and follow the evolution of the zero modes, which are always separated by a finite gap from the rest of the spectrum (see the Supplemental Material [28]).

Step I—We decouple the two very left sites $\vec{s}_1$ and $\vec{s}_3$ from the system by switching off the couplings $H^{(K)}_{\vec{s}_i,\vec{s}_j}$ on the links $\vec{s}_1 - \vec{s}_2$ and $\vec{s}_3 - \vec{s}_4$, and simultaneously couple them by switching on the hopping on the link $\vec{s}_1 - \vec{s}_3$:

$$H_I(t) = \cos\phi_t (H^{(K)}_{\vec{s}_1\vec{s}_2} + H^{(K)}_{\vec{s}_3\vec{s}_4}) + \sin\phi_t H^{(h)}_{\vec{s}_1\vec{s}_3}.$$

Following the evolution of the zero modes (see the Supplemental Material [28]), we have at the end of this step that $\gamma^{(u)}_L = -d_3$ and $\gamma^{(l)}_L = -c_3$. Note that the two decoupled sites $\vec{s}_1$ and $\vec{s}_3$ carry exactly one fermion, which has been taken out of the system.

Step II—We put now this fermion in the lower wire by switching on $H^{(K)}_{\vec{s}_3,\vec{s}_4}$ on the link $\vec{s}_3 - \vec{s}_4$, and $H^{(p)}_{\vec{s}_1,\vec{s}_3}$ on the link $\vec{s}_1 - \vec{s}_3$:

$$H_{II}(t) = H^{(h)}_{\vec{s}_1\vec{s}_3} + \sin\phi_t (H^{(p)}_{\vec{s}_1\vec{s}_3} + H^{(K)}_{\vec{s}_3\vec{s}_4}).$$

The zero modes evolve such that at the end $\gamma^{(u)}_L = c_1$ and $\gamma^{(l)}_L = -c_3$. Note that at this stage the Majorana mode $\gamma^{(u)}_L$ ($\gamma^{(l)}_L$) has already been moved from the upper (lower) to the lower (upper) wire. However, two additional steps are needed to recover the original configuration of the wires.

Step III—We move the Majorana mode from the site $\vec{s}_1$ to the site $\vec{s}_3$ by switching on $H^{(lp)}_{\vec{s}_1}$ and simultaneously switching off $H^{(K)}_{\vec{s}_1\vec{s}_3}$ on the link $\vec{s}_1 - \vec{s}_3$:

$$H_{III}(t) = \sin\phi_t H^{(lp)}_{\vec{s}_1} + \cos\phi_t H^{(K)}_{\vec{s}_1\vec{s}_3} + H^{(K)}_{\vec{s}_3\vec{s}_4}.$$

The evolution of the zero modes results in $\gamma_L^{(u)} = d_1$, while $\gamma_L^{(l)} = -c_3$ remains fixed.

Step IV—Finally, we switch off $H^{(lp)}_{\vec{s}_1}$ and switch on $H^{(K)}_{\vec{s}_1\vec{s}_2}$:

$$H_{IV}(t) = \sin\phi_t H^{(K)}_{\vec{s}_1\vec{s}_2} + H^{(K)}_{\vec{s}_3\vec{s}_4} + \cos\phi_t H^{(lp)}_{\vec{s}_1},$$

so that finally we get the desired braiding $\gamma_L^{(u)} \mapsto d_1 = \gamma_L^{(l)}$ and $\gamma_L^{(l)} \mapsto -c_1 = -\gamma_L^{(u)}$ for the left Majorana modes on the wires n and $n+1$, which corresponds (up to an unimportant phase factor) to the unitary $U_n = e^{\pi\gamma_L^{(u)}\gamma_L^{(l)}/4}$.

Note that the braiding in the other direction $U_n^\dagger$, $\gamma_L^{(u)} \mapsto -\gamma_L^{(l)}$, $\gamma_L^{(l)} \mapsto \gamma_L^{(u)}$, can be achieved by putting the uncoupled fermion in the upper (instead of the lower) wire with a simple modification of Steps II–IV.

The braiding results in the change of the correlation functions of the Majorana operators (see Fig. 2) and thus changes also the long-range fermionic correlations. This can also be translated into the change of the fermionic parities of the wires: if $|0_n\rangle$ ($|1_n\rangle$) denotes the state of the nth wire with even (odd) parity and, for example, we start from the state $|0_n 0_{n+1}\rangle$ with both wires with even parity, then the braiding U_n results in $U_n|0_n 0_{n+1}\rangle = (|0_n 0_{n+1}\rangle + |1_n 1_{n+1}\rangle)/\sqrt{2}$, and $U_n^2|0_n 0_{n+1}\rangle = |1_n 1_{n+1}\rangle$. The result of the braiding, therefore, can be checked by measuring the change of the Majorana correlation functions in time-of-flight or spectroscopic experiments [21], or by measuring the parity of the wires by counting the number of fermions modulo two [18].

Nonideal wires and nonperfect operations.—We have just demonstrated the braiding for the case of ideal Kitaev wires and perfect local operations (single site or link addressing). Remarkably, the topological origin of the Majorana modes ensures the robustness of the results of the braiding protocol based on Steps I–IV also in the realistic case of nonideal wires and local operations provided the Majorana modes are spatially well separated. We have checked this numerically by considering two nonideal wires with $J \neq |\Delta|$, $\mu \neq 0$, and assuming that the local operations have an error α in the following sense: (i) Switching on the hopping J and/or the pairing Δ on the link $(u, 1) - (l, 1)$ also introduces the hopping $J\alpha$ and/or the pairing $\alpha\Delta$ on the link $(u, 2) - (l, 2)$. (ii) Switching off the couplings on the link $(w, 1) - (w, 2)$ also reduces the couplings on the link $(w, 2) - (w, 3)$ by a factor $(1 - \alpha)$. (iii) Raising the local potential V on the site $(u, 1)$ results in a local potential αV on the neighboring sites $(u, 2)$ and $(l, 1)$. As an example, we present in Fig. 3 numerical results of the braiding protocol with errors $\alpha = 0.05$ and $\alpha = 0.1$ in the local operations for two quantum wires of the length $L = 40$ with $|\Delta| = 1.5J$ and $\mu = 0$. One can clearly see the robustness of the final results of the braiding. Note that these results also imply that the protocol

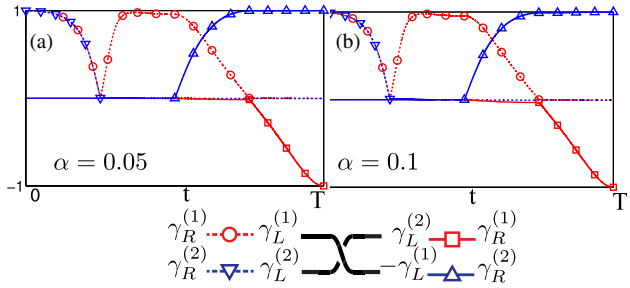

FIG. 3 (color online). Evolution of the Majorana correlation functions $\langle i\gamma_L^{(1)}\gamma_R^{(1)}\rangle$ (red circle), $\langle i\gamma_L^{(2)}\gamma_R^{(2)}\rangle$ (blue downward triangle), $\langle i\gamma_L^{(2)}\gamma_R^{(1)}\rangle$ (red square), and $\langle i\gamma_L^{(1)}\gamma_R^{(2)}\rangle$ (blue upward triangle) during the braiding protocol with errors (a) $\alpha = 0.05$ and (b) $\alpha = 0.01$ in the local operations for two nonideal quantum wires with $|\Delta| = 1.5J$ and $\mu = 0$. Markers are only drawn in regions where the correlation functions are nonzero.

works in the presence of a harmonic trap (see the Supplemental Material [28]), which also leads to an extension of the MF wave function (see Ref. [20]).

Braid group.—It is also easy to check that the braiding unitary U_n fulfills all necessary conditions of the braid group [2]: for any two neighboring braiding unitaries U_n and U_{n+1}, one has $U_n U_{n+1} \neq U_{n+1} U_n$ and $U_{n-1} U_n U_{n-1} = U_n U_{n-1} U_n$. To show this, consider three wires with left Majorana modes $\gamma_L^{(1)}$, $\gamma_L^{(2)}$, and $\gamma_L^{(3)}$, and the unitaries $U_1 = e^{\pi\gamma_L^{(1)}\gamma_L^{(2)}/4} = (\mathbb{1} + \gamma_L^{(1)}\gamma_L^{(2)})/\sqrt{2}$ and $U_2 = e^{\pi\gamma_L^{(2)}\gamma_L^{(3)}/4} = (\mathbb{1} + \gamma_L^{(2)}\gamma_L^{(3)})/\sqrt{2}$ that braid the modes $\gamma_L^{(1)}$, $\gamma_L^{(2)}$ and $\gamma_L^{(2)}$, $\gamma_L^{(3)}$, respectively. The braid group conditions, $U_1 U_2 \neq U_2 U_1$ and $U_1 U_2 U_1 = U_2 U_1 U_2$, can now be easily checked by direct multiplications.

These properties can be tested experimentally by measuring the corresponding changes of the fermionic correlation functions. For example, the action of $U_1 U_2$ results in $i\langle\gamma_L^{(1)}\gamma_R^{(1)}\rangle \mapsto i\langle\gamma_L^{(3)}\gamma_R^{(1)}\rangle$, $i\langle\gamma_L^{(2)}\gamma_R^{(2)}\rangle \mapsto -i\langle\gamma_L^{(1)}\gamma_R^{(2)}\rangle$ and $i\langle\gamma_L^{(3)}\gamma_R^{(3)}\rangle \mapsto -i\langle\gamma_L^{(2)}\gamma_R^{(3)}\rangle$, while $U_1 U_2 U_1$ produces the following changes: $i\langle\gamma_L^{(1)}\gamma_R^{(1)}\rangle \mapsto i\langle\gamma_L^{(3)}\gamma_R^{(1)}\rangle$, $i\langle\gamma_L^{(2)}\gamma_R^{(2)}\rangle \mapsto -i\langle\gamma_L^{(2)}\gamma_R^{(1)}\rangle$, and $i\langle\gamma_L^{(3)}\gamma_R^{(3)}\rangle \mapsto i\langle\gamma_L^{(1)}\gamma_R^{(3)}\rangle$ (see Fig. 4). This change in the correlation functions can be measured, for example, in TOF or spectroscopic experiments as proposed in Ref. [21].

Deutsch-Jozsa algorithm. Although the braiding of MFs is robust, it does not provide a tool to construct a universal set of gates needed for TQC: as it has been shown in Ref. [23], only a subgroup of the Clifford group can be realized via braiding. Fortunately, not all QC algorithms require a universal set of gates. One example is the Deutsch-Jozsa algorithm [24], which, as we will show below, can be implemented for two qubits in a remarkably efficient way via braiding of MFs.

The Deutsch-Jozsa algorithm allows us to determine whether the function (“oracle”) $g(x)$, which is defined on the space of states of n qubits and takes the values

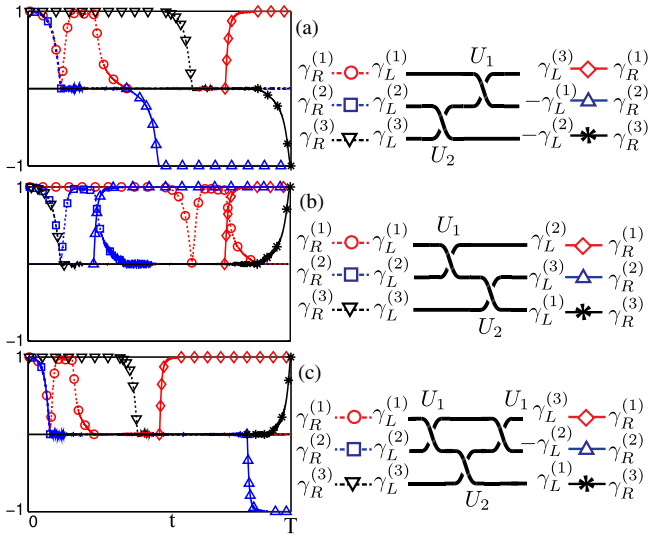

FIG. 4 (color online). Braid group in a setup of three wires. We present the real-time evolution of the correlations functions $i\langle\gamma_L^{(n)}\gamma_R^{(m)}\rangle$ under the action of (a) U_2U_1, (b) U_1U_2, and (c) $U_1U_2U_1$ for a chain of the length $L = 40$ with $|\Delta| = 1.5J$ and $\mu = 0$. Markers are only drawn in regions where the correlation functions are nonzero.

0 or 1, g: $\{|0\rangle, |1\rangle\}^{\otimes n} \mapsto \{0, 1\}$, is constant (has the same value, say, 0, for all inputs) or balanced (takes value 0 for half of the inputs, and 1 for the other half). For the algorithm to work, one needs a robust implementation of the function g (a faulty oracle spoils the quantum speedup [29]) as the unitary U_g: $|x\rangle \mapsto (-1)^{g(x)}|x\rangle$, where $|x\rangle \in \{|0\rangle, |1\rangle\}^{\otimes n}$, which is a major problem for experimental realizations.

For two qubits with the computational basis $\{|00\rangle, |01\rangle, |10\rangle, |11\rangle\}$, a possible choice for U_g is

$$U_{g_0} = \mathrm{diag}(1, 1, 1, 1), \qquad U_{g_1} = \mathrm{diag}(1, 1, -1, -1),$$
$$U_{g_2} = \mathrm{diag}(1, -1, -1, 1), \qquad U_{g_3} = \mathrm{diag}(1, -1, 1, -1),$$

for the constant g_0 and the balanced g_1, g_2, and g_3 oracle functions, respectively. (Note that an equivalent set of oracles can be obtained by multiplying the above unitaries with -1.) The algorithm works then in the following way: after preparing the system in the state $|00\rangle$, we apply the Hadamard gate H to each qubit, $H|0\rangle = (|0\rangle + |1\rangle)/\sqrt{2}$, $H|1\rangle = (|0\rangle - |1\rangle)/\sqrt{2}$, then we apply the unitary U_g corresponding to the oracle under test, then again the Hadamard gate to each qubit, and, finally, we measure the probability to find the system in the state $|00\rangle$. This probability is 1 if $g(x)$ is constant, and 0 if $g(x)$ is balanced, as can be seen from the following calculations:

$$|00\rangle \overset{H\otimes H}{\mapsto} \frac{1}{2}\sum_{\mathbf{x}}|\mathbf{x}\rangle \overset{U_g}{\mapsto} \frac{1}{2}\sum_{\mathbf{x}}(-1)^{g(\mathbf{x})}|\mathbf{x}\rangle,$$
$$\overset{H\otimes H}{\mapsto} \frac{1}{4}\sum_{\mathbf{x}}(-1)^{g(\mathbf{x})}\sum_{\mathbf{y}}(-1)^{\mathbf{x}\cdot\mathbf{y}}|\mathbf{y}\rangle, \tag{1}$$

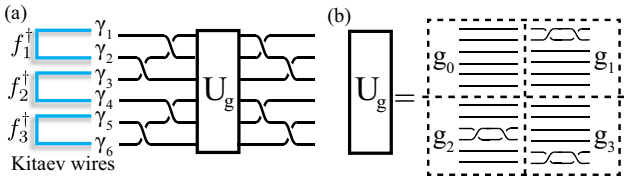

FIG. 5 (color online). (a) Setup and implementation of the oracle Deutsch-Jozsa algorithm for two qubits via braiding. (b) Implementation of the oracle unitary U_g via braiding (see main text).

where we define $\mathbf{x} = (x_1, x_2)$ and $\mathbf{y} = (y_1, y_2)$ with $x_i, y_i \in \{0, 1\}$, and $\mathbf{x}\cdot\mathbf{y} = x_1y_1 + x_2y_2$.

To implement the above algorithm, we use a setup of three quantum wires in the geometry shown in Fig. 5 and define a computational basis for two qubits as $|00\rangle = f_2^\dagger|0_f\rangle$, $|01\rangle = f_3^\dagger|0_f\rangle$, $|10\rangle = f_1^\dagger|0_f\rangle$, and $|11\rangle = f_1^\dagger f_2^\dagger f_3^\dagger|0_f\rangle$ [22]. Here $|0_f\rangle$ is the vacuum state for fermionic modes $f_i = (\gamma_i^{(L)} - i\gamma_i^{(R)})/2$, where $\gamma_i^{(L)}$ and $\gamma_i^{(R)}$ are two Majorana modes on the ith wire. Note that with three wires we encode only two qubits [30] because the braiding preserves the total fermionic parity and, therefore, all states from the computational basis must have the same parity (odd in our case).

The Hadamard gates and the oracle unitaries U_{g_i} can be implemented by noting that the braiding of Majorana modes γ_i and γ_j is equivalent to the unitary $U_{ij} = e^{\pi\gamma_i\gamma_j/4} = (\mathbb{1} - \gamma_i\gamma_j)/\sqrt{2}$: Then, it is easy to see that $H\otimes\mathbb{1} = U_{12}U_{23}U_{12}$ and $\mathbb{1}\otimes H = U_{56}U_{45}U_{56}$ for the Hadamard gates acting on the first and the second qubit, respectively, and $U_{g_1} = U_{12}^2$, $U_{g_2} = U_{34}^2$, and $U_{g_3} = U_{56}^2$ for the oracle unitaries ($U_{g_0} = \mathbb{1}$). As a result, the Deutsch-Jozsa-algorithm can be realized with 14 braiding operations. In our case, however, the number of operations can be reduced to nine: the sequence

$$\mathcal{U}_i = U_{45}U_{56}U_{23}U_{12}U_{g_i}U_{56}U_{45}U_{12}U_{23}$$

acting on $|00\rangle$ gives $\mathcal{U}_0|00\rangle = |00\rangle$ for the constant case and $\mathcal{U}_1|00\rangle = i|10\rangle$, $\mathcal{U}_2|00\rangle = |11\rangle$, and $\mathcal{U}_3|00\rangle = i|01\rangle$ for the balanced case. Note also that this protocol can be implemented in five steps because operations on the Majorana modes $\gamma_{1,2,3}$ and $\gamma_{4,5,6}$ before and after the oracle unitary U_{g_i} can be performed in parallel. The final state of the system and, therefore, the probability to find it in the state $|00\rangle$, can be determined by measuring the parities of the individual wires in a spectroscopic experiment [21] or fermionic number counting [18]. Taking into account the discussed insensitivity of the braiding to experimental imperfections, the proposed protocol provides a robust implementation of the Deutsch-Jozsa algorithm.

Conclusion.—Cold atom setups combined with local addressing provide an efficient tool to probe the non-Abelian anyonic statistics of MFs and to exploit it for TQC. By adding well-controlled though topologically

unprotected operations (e.g., the SWAP gate), one can go beyond the braid group and provide a universal "hybrid" set of gates (see also Refs. [31,32]). We will address this issue in our future work [33].

We thank I. Bloch, F. Gerbier, N. Goldman, C. Gross, Y. Hu, C. Laflamme, S. Nascimbène, and N. Yao for useful comments and discussions. This work has been supported by the Austrian Science Fund FWF (SFB FOQUS F4015-N16), the U.S. Army Research Office with funding from the DARPA OLE program, the European Commission via the integrated projects AQUTE and SIQS, and by the ERC Synergy Grant UQUAM.

[1] A. Kitaev, Ann. Phys. (Amsterdam) **303**, 2 (2003).
[2] C. Nayak, Steven H. Simon, A. Stern, M. Freedman, and S. Das Sarma, Rev. Mod. Phys. **80**, 1083 (2008).
[3] J. K. Pachos, *Introduction to Topological Quantum Computation* (Cambridge University Press, Cambridge, England, 2012).
[4] S. Das Sarma, M. Freedman, and C. Nayak, Phys. Rev. Lett. **94**, 166802 (2005).
[5] C. Zhang, V. W. Scarola, S. Tewari, and S. Das Sarma, Proc. Natl. Acad. Sci. U.S.A. **104**, 18 415 (2007).
[6] V. Mourik, K. Zuo, S. M. Frolov, S. R. Plissard, E. P. A. M Bakkers, and L. P. Kouwenhoven, Science **336**, 1003 (2012).
[7] M. T. Deng, C. L. Yu, G. Y. Huang, M. Larson, P. Caroff, and H. Q. Xu, Nano Lett. **12**, 6414 (2012).
[8] A. Das, Y. Ronen, Y. Most, Y. Oreg, M. Heiblum, and H. Shtrikman, Nat. Phys. **8**, 887 (2012).
[9] J. Alicea, Y. Oreg, G. Refael, F. von Oppen, and M. P. A. Fisher, Nat. Phys. **7**, 412 (2011).
[10] B. I. Halperin, Y. Oreg, A. Stern, G. Refael, J. Alicea, and F. von Oppen, Phys. Rev. B **85**, 144501 (2012).
[11] M. Burrello, B. van Heck, and A. R. Akhmerov. Phys. Rev. A **87**, 022343 (2013).
[12] C. W. J. Beenakker, Annu. Rev. Condens. Matter Phys. **4**, 113 (2013).
[13] F. Hassler, A. R. Akhmerov, C.-Y. Hou, and C. W. J. Beenakker, New J. Phys. **12**, 125002 (2010).
[14] K. Flensberg, Phys. Rev. Lett. **106**, 090503 (2011).
[15] M. Leijnse and K. Flensberg, Phys. Rev. B **86**, 104511 (2012).
[16] D. Pekker, C.-Y. Hou, V. Manucharyan, and E. Demler, Phys. Rev. Lett. **111**, 107007 (2013).
[17] J. Simon, W. S. Bakr, R. Ma, M. E. Tai, P. M. Preiss, and M. Greiner, Nature (London) **472**, 307 (2011).
[18] J. F. Sherson, C. Weitenberg, M. Endres, M. Cheneau, I. Bloch, and S. Kuhr, Nature (London) **467**, 68 (2010).
[19] L. Jiang, T. Kitagawa, J. Alicea, A. R. Akhmerov, D. Pekker, G. Refael, J. I. Cirac, E. Demler, M. D. Lukin, and P. Zoller, Phys. Rev. Lett. **106**, 220402 (2011).
[20] S. Nascimbène, J. Phys. B **46**, 134005 (2013).
[21] C. V. Kraus, S. Diehl, M. A. Baranov, and P Zoller, New J. Phys. **14**, 113036 (2012).
[22] C. Nayak and F. Wilczek, Nucl. Phys. **B479**, 529 (1996).
[23] A. Ahlbrecht, L. S. Georgiev, and R. F. Werner. Phys. Rev. A **79**, 032311 (2009).
[24] D. Deutsch and R. Jozsa, Proc. R. Soc. A **439**, 553 (1992).
[25] A. Y. Kitaev, Phys. Usp. **44**, 131 (2001).
[26] C. Weitenberg, M. Endres, J. F. Sherson, M. Cheneau, P. Schauß, T. Fukuhara, I. Bloch, and S. Kuhr, Nature (London) **471**, 319 (2011).
[27] T. Fukuhara, A. Kantian, M. Endres, M. Cheneau, P. Schauß, S. Hild, D. Bellem, U. Schollwöck, T. Giamarchi, C. Gross, I. Bloch, and S. Kuhr, Nat. Phys. **9**, 235 (2013).
[28] See Supplemental Material at http://link.aps.org/supplemental/10.1103/PhysRevLett.111.203001 for details on the evolution of the zero modes and the gaps during the braiding, as well as a discussion of the effect of an external harmonic trapping potential on the braiding protocol.
[29] O. Regev and L. Schiff, *Proceedings of 35th International Colloquium on Automata, Languages and Programming of ICALP, Reykjavik-Iceland 2008* (Springer, New York, 2008).
[30] L. S. Georgiev. Phys. Rev. B **74**, 235112 (2006).
[31] D. J. Clarke, J. D. Sau, and S. Tewari, Phys. Rev. B **84**, 035120 (2011).
[32] J. D. Sau, S. Tewari, and S. Das Sarma, Phys. Rev. A **82**, 052322 (2010).
[33] C. Laflamme, M. Baranov, P. Zoller, and C. Kraus (to be published).